

Short communication

The ray-tracing mapping operator in an asymmetric atmosphere

Zhenjie Hong^{a,b,*}, Fan Ye^b, Peng Guo^a

^a Shanghai Astronomical Observatory, Chinese Academy of Sciences, Shanghai 200030, China

^b School of Mathematics & Information Science, Wenzhou University, Wenzhou 325027, China

Received 21 May 2007; received in revised form 11 June 2007; accepted 15 June 2007

Abstract

In a spherically symmetric atmosphere, the refractive index profile is retrieved from bending angle measurements through Abel integral transform. As horizontal refractivity inhomogeneity becomes significant in the moist low atmosphere, the error in refractivity profile obtained from Abel inversion reaches about 10%. One way to avoid this error is to directly assimilate bending angle profile into numerical weather models. This paper discusses the 2D ray-tracing mapping operator for bending angle in an asymmetric atmosphere. Through simulating computations, the retrieval error of the refractivity in horizontal inhomogeneity is assessed. The step length of 4 rank Runge–Kutta method is also tested.

© 2007 National Natural Science Foundation of China and Chinese Academy of Sciences. Published by Elsevier Limited and Science in China Press. All rights reserved.

Keywords: GPS occultation; Ray-tracing; Data assimilation; Runge–Kutta method

1. Introduction

In recent years, the technique of global positioning system/low earth orbit (GPS/LEO) radio occultation has opened up a new route for exploring the earth atmosphere. After successful occultation observations of project GPS/MET (launched by US in 1995), satellites Orsted (launched by Denmark in 1999), SAC-C (launched by Argentina and US in 2000) and CHAMP (launched by Germany in 2000), the six satellites system COSMIC (joint project of Taiwan of China and US launched in 2006 April) followed. The LEO system nowadays can provide about 3000 global distributed occultation observations each day. The GPS/LEO radio occultation technique can provide high-accuracy, high-resolution and global coverage profiles of the earth's ionosphere and neutral atmosphere. The occultation technique is proved to possess advantages of being all-weather,

and free of secular systematic drift low-cost, global coverage, high-accuracy and high-resolution [1]. The technique of assimilating GPS occultation data into numerical weather prediction and global analysis provides a new potentially valuable data method for meteorological and atmospheric sciences.

How to effectively assimilate GPS occultation data into numerical weather prediction has attracted special concern in recent years. Kuo et al. [2] investigated some assimilation methods for occultation data and believed that the refractive and bending angle assimilations were possibly the available approaches. Zou et al. [3] analyzed the role possessed by the assimilation of GPS refractivity data into MM5 four-dimensional variation in improving the performance of the model. Kuo [4] designed a set of simulative experiments of occultation observations and evaluated the effects of the refractivity assimilation of occultation data in storm weather prediction. Using 1D-VAR technique, Kursinski et al. [5] assimilated GPS/MET refractive data into global analysis of European Center for medium range weather forecasting (ECMWF). Healy and Eyre [6] simulated and tested the same scheme. As a 1D-VAR prob-

* Corresponding author. Address: Shanghai Astronomical Observatory, Chinese Academy of Sciences, Shanghai 200030, China. Tel.: +86 577 88663100; fax: +86 577 86689528.

E-mail address: hong@wzu.edu.cn (Z. Hong).

lem, Palmer et al. [7,8] and Liu et al. [9] discussed the validation of Abel integral operator in the bending angle assimilation in occultation data precession. Engeln et al. [10] tested the sensitivity of the bending angle inversion via Abel integral operator in 1D-VAR. Zou et al. [11,12] and Liu et al. [13] assimilated the bending angle data from GPS/MET experiment using a ray-tracing operator. Based on a 2D ray-tracing operator method, Zou et al. [14] analyzed statistically the bending angle errors in spherically symmetrical atmospheric modes. Shao and Zou [15] studied the sensitivity of retrieved atmosphere on the reference fields and their characteristics.

In a spherically symmetric atmosphere, the refractive index profile can be retrieved from bending angle measurements through Abel integral transform. As horizontal refractivity inhomogeneity becomes significant in the moist low atmosphere [16,17], the error in refractivity profile introduced from Abel inversion reaches about 10%. One way to avoid this error is to directly assimilate bending angle profile into numerical weather models [11–13], but it consumes computer time.

This paper introduces a 2D ray-tracing mapping operator for bending angle in an asymmetric atmosphere. Based on simulating computations, the retrieval error from the refractivity horizontal inhomogeneity is assessed. The step length of 4 rank Runge–Kutta method is tested. The result shows that by reasonably adjusting the integral step it is possible to save nearly an order of magnitude of computing time and to preserve a requisite accuracy, and accordingly a higher computing efficiency may be achieved.

2. Data variational assimilation

In case that the temperature and water vapor are simultaneously retrieved from the occultation data, the problem of fuzziness will arise in mathematics. In dealing with fuzziness problem, to improve the retrieve accuracy, Eyre [18] proposed the one-dimensional (1D) variational assimilation retrieval technique.

One of the basic assumptions in variational assimilation technique is that the maximum likelihood value of the atmospheric state vector \mathbf{x} satisfies that the value function $J(\mathbf{x})$ is the minimum [19]

$$J(\mathbf{x}) = \frac{1}{2}(\mathbf{x} - \mathbf{x}^b)^T \mathbf{B}^{-1}(\mathbf{x} - \mathbf{x}^b) + \frac{1}{2}(\mathbf{y}^0 - H\{\mathbf{x}\})^T (\mathbf{O} + \mathbf{F})^{-1}(\mathbf{y}^0 - H\{\mathbf{x}\}) + J_c(\mathbf{x}) = \min, \quad (1)$$

where \mathbf{x}^b is the state vector of the background field; \mathbf{y}^0 is the observation vector; \mathbf{B} is the error expectation covariance matrix of the state vector of the background field; $H\{\mathbf{x}\}$ is the observation operator, which maps the state vector \mathbf{x} into the observation vector space; \mathbf{O} is the error expectation covariance matrix of the observation vector; \mathbf{F} is the error expectation covariance matrix of the observation operator, and $J_c(\mathbf{x})$ is the additional penalty function,

usually representing other dynamical or physical constraints in the system.

In the 2D variational assimilation problem of the bending angle data of an asymmetric atmosphere, the observation vector \mathbf{y}^0 is the observed bending angle series in the form of a function of the impact parameters. The observation operator $H\{\mathbf{x}\}$ is expressed to be a 2D ray-tracing mapping operator, which maps state vector \mathbf{x} into the bending angle series shown as the function of impact parameters.

3. 2D ray-tracing mapping operator

From the accurately known GPS and LEO ephemeris and atmospheric state vectors, using a ray-tracing technique, it is possible to obtain the trace of signal, and accordingly, the series of bending angle and the corresponding impact parameter [20–22]. However, it costs much computer time, and is difficult to use in real-time applications. Zou et al. [11] developed a 2D ray-tracing operator, and Liu and Zou [23] improved the accuracy and efficiency of the 2D ray-tracing operator.

The 2D ray-tracing operator involves two parts:

- (i) The atmospheric refractivity may be obtained from the Smith–Weitraub equation

$$N = (n - 1) \times 10^6 = \frac{77.6}{T} \left(P + 4810 \frac{P_w}{T} \right), \quad (2)$$

where n and N are refractive index and refractivity, respectively; p and p_w are the overall atmosphere pressure and partial water vapor pressure (hPa), respectively; T is the absolute temperature (K).

- (ii) The tracing equation of GPS signal path may be described by the second order differential equation [11,23]

$$\frac{d^2 \mathbf{u}}{ds^2} = n \nabla n. \quad (3)$$

Here, $\mathbf{u} = \mathbf{u}(s) = (x(s), y(s))^T$ is the ray trace, and s is a scale optical length of the ray trace and satisfies differential variable $ds = dL/n$, where L is the ray length. The tracing Eq. (3) is equivalent to the first order differential equations

$$\begin{cases} \frac{d\mathbf{u}}{ds} = \mathbf{v}(s) \\ \frac{d\mathbf{v}}{ds} = n \nabla n \end{cases}, \quad (4)$$

where $\mathbf{v} = d\mathbf{u}/ds$, whose boundary condition is determined from initial values of \mathbf{u} and \mathbf{v} .

The 2D ray-tracing method is shown geometrically in Fig. 1. The initial condition $\frac{d\mathbf{u}}{ds}|_{s=0}$ at occultation point of GPS ray-tracing Eq. (3) is known. The ray trace and bending angles γ , β are obtained by means of 4 ranks Runge–Kutta numerical integration method. The integral will start from the occultation point at horizontal direction toward both sides forward to the height of GPS (about 20,200 km) and backward to the height of LEO (about

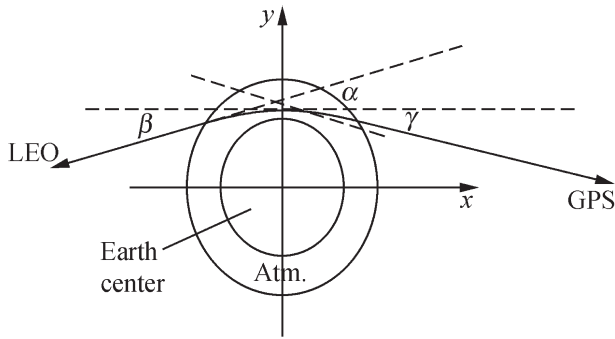


Fig. 1. Geometry of the 2D ray-tracing method.

800 km). Finally, the bending angle of signal path between GPS and LEO can be written as $\alpha = \beta + \gamma$.

4. Numerical simulation for refractivity

In an ideal atmosphere, the refractive index can be written as [25]

$$n(z, \theta) = n_0 \exp(-z/H) \cdot [1 + \mu f((z/\varepsilon + r_e|\theta|)/d)] \quad (5)$$

and its partial derivatives n'_x, n'_y are obtained by

$$n'_x = \frac{xn'_r}{r} - \frac{yn'_\theta}{r^2}, \quad n'_y = \frac{yn'_r}{r} + \frac{xn'_\theta}{r^2} \quad (6)$$

where $n(z, \theta)$ is refractive index at field point (z, θ) ; $r_e = 6370$ km (Earth radius); $z = r - r_e$ (the height above surface); $r = \sqrt{x^2 + y^2}$ and $\theta = \arctan(x/y)$ are the Earth center distance and central angle, respectively; $n_0 = 300$, $H = 7.5$ km, $\varepsilon = 0.1$, $d = 100$ km, $\mu = 0.1$, and

$$f(\xi) = \begin{cases} 1 & \xi > 1 \\ \sin(\frac{\pi\xi}{2}) & -1 \leq \xi \leq 1 \\ -1 & \xi < -1 \end{cases}$$

From the model values at grid points, n'_r, n'_θ may be obtained via logarithm spline interpolation in vertical direction and via linear spline interpolation in horizontal direction. The values of n'_x, n'_y are then obtained from Eq. (6).

From Eq. (5), the atmospheric refractivity $N(z, \theta)$ can be expressed as a function of surface height z and central angle θ . The distribution of refractivity $N(z, \theta)$ below 10 km is shown in Fig. 2, which shows that refractivity increases with the rising central angle θ . Therefore, the problem of non-homogeneity arises below certain height. The horizontal gradient of refractivity on the right is greater than that on the left. However, the horizontal gradient of refractivity approaches 0 as the surface height reaches 10 km.

5. Comparison of 2D ray-tracing mapping operator and 1D Abel integral transformation for bending angle

In a spherically symmetric atmosphere, the bending angle profile may be obtained from refractive index profile via Abel integral transformation [26]

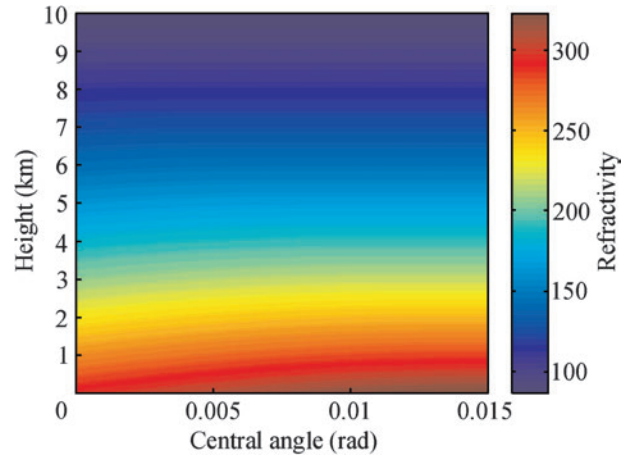


Fig. 2. Diagram of refractivity below 10 km.

$$\alpha = 2 \int_{r_1}^{\infty} dx = 2a \int_{r_1}^{\infty} \frac{1}{\sqrt{n^2 r^2 - a^2}} \frac{d \ln(n)}{dr} dr, \quad (7)$$

where r is the distance from field-point to the center of the Earth's local atmospheric curvature, and

$$a = n(r) \cdot r$$

is defined as the impact parameter.

Palmer et al. [7,8] and Liu et al. [9] deduced the bending angle profiles via Abel integral transformation in a spherically symmetric atmosphere. The error will arise in the above method if there is atmospheric refractivity non-homogeneity at horizontal direction. In order to estimate the error, the results of α_{2D} (via 2D ray-tracing mapping operator) and α_{1D} (via Abel integral transformation) are compared from simulation formula for refractive index in the ideal atmospheric model. The results of relative error $\frac{\alpha_{1D} - \alpha_{2D}}{\alpha_{2D}}$ are shown in Fig. 3, which reveals that the relative error of α_{2D} and α_{1D} may reach 14% in the region where a rather greater horizontal gradient of refractive index appears.

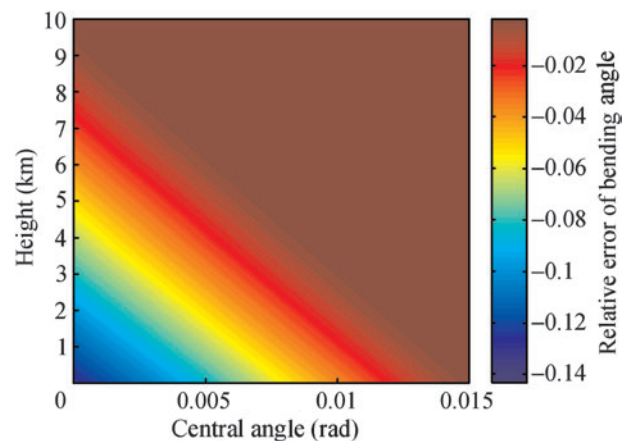


Fig. 3. The relative error of α_{2D} and α_{1D} .

6. The relative error of Abel transformation in an asymmetric atmosphere

In a spherically symmetric atmosphere, the atmospheric refractive index profile $n(r)$ may be obtained from bending angle profiles using Abel inverse transformation [27]

$$n(a) = \exp\left(\frac{1}{\pi} \int_a^\infty \frac{\alpha(\xi)}{\sqrt{\xi^2 - a^2}} d\xi\right) \tag{8}$$

and the refractivity is written as

$$N = (n - 1) \times 10^6 \tag{9}$$

and the altitude is

$$h = \frac{a}{n(a)} - r_c, \tag{10}$$

where r_c is the local curvature radius of the Earth and a is the impact parameter.

In order to testify the refractivity error from Abel inverse transformation introduced by non-homogeneity atmosphere in horizontal direction, first, a 2D ray-tracing method is used to calculate bending angle series; second, Abel inverse transformation (8) is used to obtain N_{2D} ; finally, spline interpolation is used to get refractivity series N at the same altitude from N_{2D} . The resulted relative error $\frac{N_{2D}-N}{N}$ is shown in Fig. 4, which means that, the relative error from Abel inverse transformation retrieval may reach 6% in a refractivity horizontal non-homogeneity environment.

7. Testing for integral step of Runge–Kutta method

One of the most troublesome problems for GPS bending angle data variational assimilation is extremely great quantity of operation [11]. To ensure a higher computing efficiency within the allowable accuracy range, it is necessary to find a reasonable integral step in Runge–Kutta method [24]. Put the initial steps being 0.01 km (0–10 km), 0.1 km (10–50 km) and 1 km (above 50 km), respectively, and

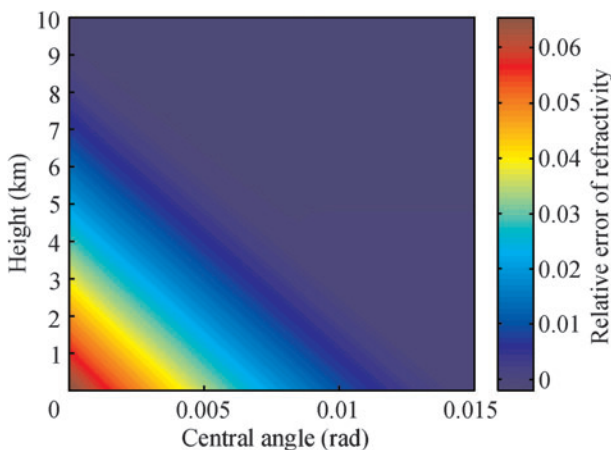


Fig. 4. The relative error of N_{2D} and N .

Table 1
Testing for integral step of Runge–Kutta method

Height (km)	Step (km)	Bending angle (rad)	Relative error (%)
1	0.01	2.289387×10^{-2}	0
	0.64	2.291755×10^{-2}	0.107
	1.28	2.294305×10^{-2}	0.229
	2.56	2.299248×10^{-2}	0.431
	5.12	2.309318×10^{-2}	0.871
	10.24	2.329512×10^{-2}	1.753
10	0.1	6.564257×10^{-3}	0
	1.6	6.573498×10^{-3}	0.141
	3.2	6.584061×10^{-3}	0.302
	6.4	6.605436×10^{-3}	0.627
	12.8	6.647705×10^{-3}	1.271
30	1	4.483706×10^{-4}	0
	16	4.491915×10^{-4}	0.183
	32	4.5011377×10^{-4}	0.389
	64	4.5210145×10^{-4}	0.832
	128	4.5663614×10^{-4}	1.843

gradually increase the integral steps. In Table 1, the results of bending angles are listed and compared with the initials.

Based on the data of Table 1, it looks reasonable to let the integral step of Runge–Kutta be 5 km (0–10 km), 10 km (10–50 km), 60 km (above 50 km), respectively. These choices may ensure the relative errors of GPS bending angle data variational assimilation within allowable error range (<1%).

8. Summary

The horizontal inhomogeneity of refractivity in the moist low atmosphere is one of the main reasons in GPS occultation standard inversion technique.

Based on the 2D ray-tracing mapping operator, by directly assimilating the original observation data of bending angle, it may be effective to solve the problem of the retrieval error coming from horizontal inhomogeneity of refractivity. However, a large amount of computer time is required to assimilate occultation data of bending angle based on the 3D-Var technique, and the computing time is about 2–3 orders of magnitude higher than that of refractivity variational assimilation [12]. It looks reasonable to achieve better effects by combining appropriate operators to assimilate occultation data (the refractivity operator is used at upper atmosphere where atmospheric refractivity is uniform horizontally [6,19], and the ray-tracing mapping operator is used at lower atmosphere where atmospheric refractivity is nonuniform horizontally). It may be possible to save much computing time and retain the same accuracy as that of bending angle if integral step of Runge–Kutta integral method is adjusted properly. In addition, Sokolovskiy et al. [25] put forward a linearized observation operator for assimilation of radio occultation data to reduce an order of magnitude of computing time in comparison with that of bending angle assimilation, and to solve effectively the problem of the retrieval error coming from horizontal inhomogeneity of refractivity in lower atmosphere. In

GPS/LEO occultation data assimilation process, it is an important consideration to make a comprehensive survey of all kinds of assimilation operators and assimilation scheme to optimize both the computing accuracy and the quantity of operation.

Acknowledgements

This work was supported by National Natural Science Foundation of China (Grant No. 40605012), Natural Science Foundation of Zhejiang Province (Grant No. Y506040), Science and Technology Planning Project of Wenzhou Municipal (Grant No. S20060025).

References

- [1] Hajj GA, Ao CO, Iijima BA, et al. CHAMP and SAC-C atmospheric occultation results and intercomparisons. *J Geophys Res* 2004;109(D06):109.
- [2] Kuo YH, Sokolovskiy SV, Anthes RA, et al. Assimilation of GPS radio occultation data for numerical weather prediction. *Terrestrial Atmos Ocean Sci* 2000;11(1):157–86.
- [3] Zou X, Kuo YH, Guo YR. Assimilation of atmospheric radio refractivity using a nonhydrostatic mesoscale model. *Mon Wea Rev* 1995;123:2229–49.
- [4] Kuo YH, Zou X, Huang W. The impact of GPS data on the prediction of an extratropical cyclone: an observing system simulation experiment. *Dyn Atmos Ocean* 1997;27:439–70.
- [5] Kursinski ER, Healy SB, Romans LR. Initial results of combining GPS occultations with ECMWF global analyses within a 1D-Var framework. *Earth Planets Space* 2000;52:885–92.
- [6] Healy SB, Eyre J. Retrieving temperature, water vapour and surface pressure information from refractive index profiles derived by radio occultation: a simulation study. *Q J R Meteorol Soc* 2000;126:1661–83.
- [7] Palmer PI, Barnett JJ, Eyre JR, et al. A nonlinear optimal, estimation inverse method for radio occultation measurements of temperature, humidity, and surface pressure. *J Geophys Res* 2000;105(D13):17513–26.
- [8] Palmer PI, Barnett JJ. Application of an optimal estimation inverse method GPS/LEO bending angle observations. *J Geophys Res* 2001;106(D15):17147–60.
- [9] Liu M, Guo P. GPS occultation radio symmetrical model on assimilation of bending angle. *Ann Shanghai Observ Acad Sin* 2005;26:39–47, [in Chinese].
- [10] Engeln AV, Nedoluha G, Kirchengast G, et al. One-dimensional variational (1-D Var) retrieval of temperature, water vapor, and a reference pressure from radio occultation measurements: a sensitivity analysis. *J Geophys Res* 2003;108(D11):4337.
- [11] Zou X, Vandenberghe F, Wang B, et al. A ray-tracing operator and its adjoint for the use of GPS/MET refraction angle measurements. *J Geophys Res* 1999;104(D18):22301–18.
- [12] Zou X, Wang B, Liu H, et al. Use of GPS/MET refraction angle in 3D variational analysis. *Q J R Meteorol Soc* 2000;126:3013–40.
- [13] Liu H, Zou X, Shao H, et al. Impact of 837 GPS/MET bending angle profiles on assimilation and forecasts for the period June 20–30, 1995. *J Geophys Res* 2001;106(D23):31771–86.
- [14] Zou X, Liu H, Anthes RA. A statistical estimate of errors in the calculation of radio occultation bending angles caused by a 2-D approximation of raytracing and the assumption of spherical symmetry of the atmosphere. *J Atmos Ocean Tech* 2000;19:51–64.
- [15] Shao H, Zou X. The impact of observational weighting on the assimilation of GPS/MET bending angle. *J Geophys Res* 2002;107(D23):4717.
- [16] Healy SB. Radio occultation bending angle and impact parameter errors caused by horizontal refractive index gradients in the troposphere: a simulation study. *J Geophys Res* 2001;106(D11):11875–89.
- [17] Ahmad B, Tyler GL. Systematic errors in atmospheric profiles obtained from Abelian inversion of radio occultation data: effects of large-scale horizontal gradients. *J Geophys Res* 1999;104(D4):3971–92.
- [18] Eyre J. Assimilation of radio occultation measurements into a numerical weather prediction system. England: ECMWF Tech Memo; 1994, 199.
- [19] Hong ZJ, Guo P. One-dimensional variational retrieval of refractivity profiles by GPS occultation. *Chin Astron Astrophys* 2006;30:330–41.
- [20] Guo P, Hong ZJ, Yan HJ, et al. Introduction of occultation simulation software SHAOOS. *Ann Shanghai Observ Acad Sin* 2003;24:150–6, [in Chinese].
- [21] Li SY, Wang B. The time-saving numerical method for GPS/MET observation operator and its parallel computing. *Chin J Comput Phys* 2001;6:491–5, [in Chinese].
- [22] Li SY, Wang B. The time-saving numerical method for GPS/MET observation operator. *Prog Nat Sci* 2001;11(11):1186–91, [in Chinese].
- [23] Liu H, Zou X. Improvements to a forward GPS raytracing model and their impacts on assimilation of bending angle. *J Geophys Res* 2003;108(D17):4548.
- [24] Press WH, Flannery BP, Teukolsky SA, et al. Numerical recipes: the art of scientific computing. 2nd ed. Cambridge: Cambridge University Press; 1992, p. 205–214.
- [25] Sokolovskiy S, Kuo YH, Wang W. Assessing the accuracy of a linearized observation operator for assimilation of radio occultation data: case simulations with a high-resolution weather mode. *Mon Wea Rev* 2005;133(8):2200–12.
- [26] Born M, Wolf E. Principles of optics. 6th ed. Tarrytown, NY: Pergamon; 1980, p. 165–168.
- [27] Fjeldbo G, Kliore AJ, Eshleman VR. The neutral atmosphere of Venus as studied with the Mariner V radio occultation experiments. *Astronom J* 1971;76:123–40.